International Journal of Pressure Vessels and Piping 110 (2013) 66–71

Contents lists available at SciVerse ScienceDirect

International Journal of Pressure Vessels and Piping

journal homepage: www.elsevier.com/locate/ijpvp

Time-dependent crack growth behavior for a SMAW weldment of Gr. 91 steel

Woo-Gon Kim [a,*], Jae-Young Park [b], Hyeong-Yeon Lee [a], Sung-Deok Hong [a], Yong-Wan Kim [a], Seon-Jin Kim [c]

[a] Korea Atomic Energy Research Institute, 989-111, Daedeok-daero, Yuseong-gu, Daejeon 305-353, Republic of Korea
[b] Department of Mechanical Design Engineering, Pukyong National University, Busan 608-739, Republic of Korea
[c] Department of Mechanical & Automotive Engineering, Pukyong National University, Busan 608-739, Republic of Korea

Keywords:
Creep
C_* parameter
Creep crack growth
Gr. 91 steel
Shield metal arc weld
Weld metal
Heat affected zone

A B S T R A C T

This paper presents the experimental results on creep crack growth (CCG) behavior for BM, WM and HAZ in the weldment of Gr.91 steel, which was prepared by a shield metal arc weld (SMAW) process. A series of CCG data was obtained by the creep and creep crack growth tests under different applied loads for BM, WM and HAZ in Gr. 91 welded joint at 600 °C. The CCG behaviors were characterized by the empirical equation of the da/dt vs. C^* fracture parameter, and the CCG laws for the BM, WM and HAZ were constructed and compared, respectively. Results showed that for a given value of C^*, the WM and HAZ were almost equal, but they were about two-times faster in the CCGR curves than the BM. This reason is that the CCGRs were closely attributed to their creep strength and creep strain rates. It is thus supposed that creep cracks will dominantly initiate in the HAZ, because lower creep strength existed in the HAZ compared with BM.

1. Introduction

High-chromium steels are widely used in recent fossil power plants because of their excellent high temperature strength. In particular, modified 9Cr–1Mo steel (ASME grade 9Cr–1Mo, hereafter Gr.91) is regarded as a promising candidate for structural materials of Generation-IV reactor types such as steam generators, intermediate heat exchangers and hot pipes in sodium-cooled fast reactors (SFR), and pressure vessels in very high temperature reactors (VHTR) [1,2].

Their structural components are designed to last for up to 60 years at elevated temperatures and are often subjected to non-uniform stress and temperature distribution during service. These conditions may generate localized creep damage and propagate the cracks and ultimately may cause a fracture. A significant portion of their lives will be spent during crack propagation [3–7]. It is therefore necessary to evaluate creep crack growth (CCG) behavior during creep loading for design and safety assessment of the components, especially for Type-IV cracking of a heat affected zone (HAZ) in weldments of high-Cr ferrite and martensite (FM) steels. It is known that 9Cr or 12Cr steel tends to fail with Type-IV cracking at welded joints, resulting in shorter plant life than expected. To prevent such unexpected failures, an accurate residual life assessment method for the welded joints is required. Welded joints are considered as the composite structure of different materials consists of base metal (BM), weld metal (WM), and HAZ. Since the inhomogeneity among those materials affects the state of stress field or strain rate field near the weld fusion line and near the BM/HAZ interface, it is not easy to estimate the crack propagation behavior at the welded joint. Also, it is concerning that the difference in creep deformation properties among the BM, WM, and HAZ may bring about a difficulty in the crack assessment process [8–11]. Therefore, it is necessary to clarify the creep crack growth (or creep crack propagation) laws through experimental CCG tests for the weld joint of Gr. 91 steel.

This paper is a comparative investigation on time-dependent creep crack growth behaviors for BM, WM, and HAZ in the weldment of Gr. 91, which is prepared using a shielded metal arc weld (SMAW) process. Creep crack growth laws for the BM, WM, and HAZ are constructed using a C^* fracture parameter and the results are discussed.

2. Experimental procedures

2.1. Material and weld method

The Gr. 91 steel used in this study was a commercial type hot rolled plate 32 mm in thickness. Heat treatment conditions were

* Corresponding author.
E-mail address: wgkim@kaeri.re.kr (W.-G. Kim).

0308-0161/$ – see front matter © 2013 Elsevier Ltd. All rights reserved.
http://dx.doi.org/10.1016/j.ijpvp.2013.04.024

Table 1
Chemical composition of the G91 steel (wt.%).

C	Si	Mn	P	S	Ni	Cr	Mo	Cu	V	Al	N	Nb
0.115	0.23	0.415	0.012	0.0014	0.22	8.9	0.869	0.038	0.194	0.020	0.0513	0.073

normalized and tempered at 1050 °C/1 mim/mm and 770 °C/3 mim/mm. Chemical composition is listed in Table 1. The groove shape of the welding of two plates was designed as a single V-groove with 60°. Welded blocks were prepared by using the shielded metal arc welding process. The filler metal, CM-9Cb (brand name), was manufactured by Kobe steel as AWS Class, E9016-G (3.2–4.0 mm). The post weld heat treatment was maintained for 255 min at 750 °C.

A photo of a piece of weld block is shown in Fig. 1. The variations of Micro-Vickers hardness for the BM, WM and HAZ regions in the welded joint were measured, as shown in Fig. 2. The thickness of the HAZ region was around 3.0–5.0 mm. The hardness of the WM region showed higher values than that of the BM and HAZ regions, and in particular, the hardness in the HAZ decreased significantly by softening. This HAZ will be very weak from cracks compared with the BM and WM, and it will initiate Type-IV crack in fine-grained zone which is located in the HAZ adjacent to the parent metal. It is known that the Type-IV cracks are parallel or offset from the fusion line.

2.2. Tensile, creep and CCG tests

To obtain the material properties for the BM, WM, and HAZ regions, the tensile and creep tests were performed at 600 °C. The HAZ specimens were cut out toward the transverse direction against the welding direction (longitudinal direction) in the welded block. The tensile specimens had a rectangular cross section of 2 mm in thickness and 6.25 mm in width, with a 25 mm gauge length. The strain rate was conducted with 1×10^{-4}/s at 600 °C. The creep specimens had a cylindrical shape with a 30 mm gauge length and 6 mm diameter. The HAZ specimens position the HAZ location at the center of gage length. Using constant load creep machines of a dead-weight type with lever ratio of 20:1, creep tests were carried out with different stress levels at 600 °C. Creep strain data with elapsed times were taken automatically by a PC through a high precision LVDT. The steady state creep rate was measured from the secondary creep region of experimental creep curves. The experimental procedures for the creep tests followed the recommendations of the ASTM standard E139 [12]. From these tensile and creep tests, the material constants of D, m, A, and n were obtained for the BM, WM, and HAZ samples.

The CCG tests for the BM, WM, and HAZ samples were carried out at a constant load with different applied load levels at 600 °C. Compact tension (CT) specimens had a width (W) of 25.4 mm, a thickness (B) of 12.7 mm, and side grooves of a 10% depth. The initial crack ratio (a/W) was about 0.5, and the pre-cracking size was 2.0 mm and was machined by an electric discharge machining (EDM) technique to introduce a sharp crack tip starter for the BM, WM, and HAZ regions. In the welded joint, sharp pre-cracks for the HAZ were taken to conform to one of the HAZ locations, as shown in Fig. 3, which is an overview on the BM, WM and HAZ regions of a welded joint in a CT specimen. Load-line displacement was measured using a linear gauge assembly attached to the specimen, and the crack length was determined using the direct current potential drop (DCPD) method. Crack extension data was continuously collected using a data acquisition system. All of the experimental procedures followed the recommendations of the ASTM standard E1457 [13].

After the CCG testing, the CT specimens were broken open at liquid nitrogen temperature to measure the actual crack length, as shown in Fig. 4. The actually measured final crack length (a_{mf}) was calculated from measurements made on the fracture surface at nine equally spaced points (so-called "nine points method") using the enlarged photo of the fractured surfaces, because the individual measurements on the fracture surface vary due to crack front irregularities.

In addition, the predicted crack length (a_p) by DCPD technique was calculated by Johnson's formula:

$$\frac{a_p}{W} = \frac{2}{\pi}\cos^{-1}\left[\frac{\cosh(\pi Y_o/2W)}{\cosh\left[\frac{V}{V_o}\cosh^{-1}\left\{\frac{\cosh\pi Y_o/2W}{\cosh\pi a_o/2W}\right\}\right]}\right] \quad (1)$$

where a_o = initial crack size (reference crack size for the reference voltage V_o), Y_o = the half distance between the output voltage loads, V = the output voltage, and W = the width of specimen. The a_p was compensated by the potential measurement error and became the corrected crack length a:

$$a = \frac{a_{mf} - a_o}{a_{pf} - a_o}(a_p - a_o) + a_o \quad (2)$$

where a_{pf} is the predicted value of the final crack length.

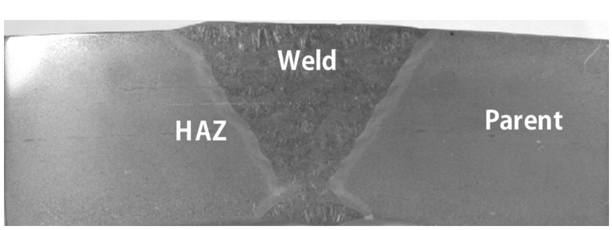

Fig. 1. Photo of a welded block.

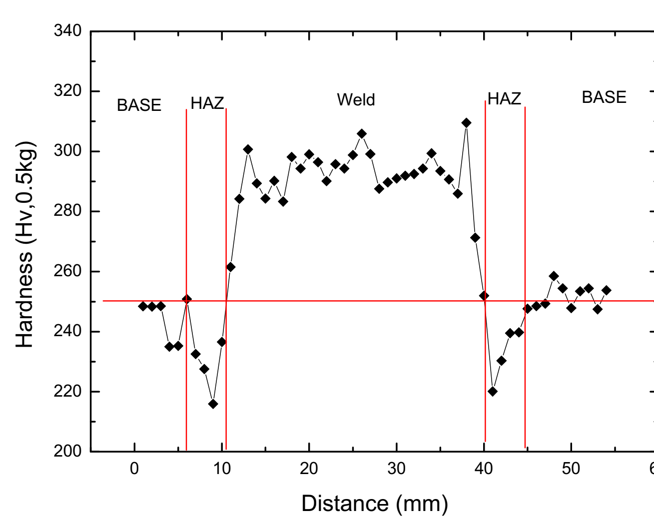

Fig. 2. Vickers hardness for weld joint of Gr. 91 steel.